AIP Applied Physics Letters

Vanadium-doped indium tin oxide as hole-injection layer in organic light-emitting devices

T.-H. Chen, Y. Liou, T. J. Wu, and J. Y. Chen

Citation: Applied Physics Letters **87**, 243510 (2005); doi: 10.1063/1.2137892
View online: http://dx.doi.org/10.1063/1.2137892
View Table of Contents: http://scitation.aip.org/content/aip/journal/apl/87/24?ver=pdfcov
Published by the AIP Publishing

Articles you may be interested in
Efficient and reliable green organic light-emitting diodes with Cl2 plasma-etched indium tin oxide anode
J. Appl. Phys. **112**, 013103 (2012); 10.1063/1.4731713

Effects of metal-doped indium-tin-oxide buffer layers in organic light-emitting devices
J. Appl. Phys. **99**, 114515 (2006); 10.1063/1.2198932

Rhodium-oxide-coated indium tin oxide for enhancement of hole injection in organic light emitting diodes
Appl. Phys. Lett. **87**, 072105 (2005); 10.1063/1.2012534

Enhancement of hole injection using iridium-oxide-coated indium tin oxide anodes in organic light-emitting diodes
Appl. Phys. Lett. **86**, 133504 (2005); 10.1063/1.1894605

Enhancement of organic light-emitting device performances with Hf-doped indium tin oxide anodes
Appl. Phys. Lett. **85**, 2092 (2004); 10.1063/1.1790026

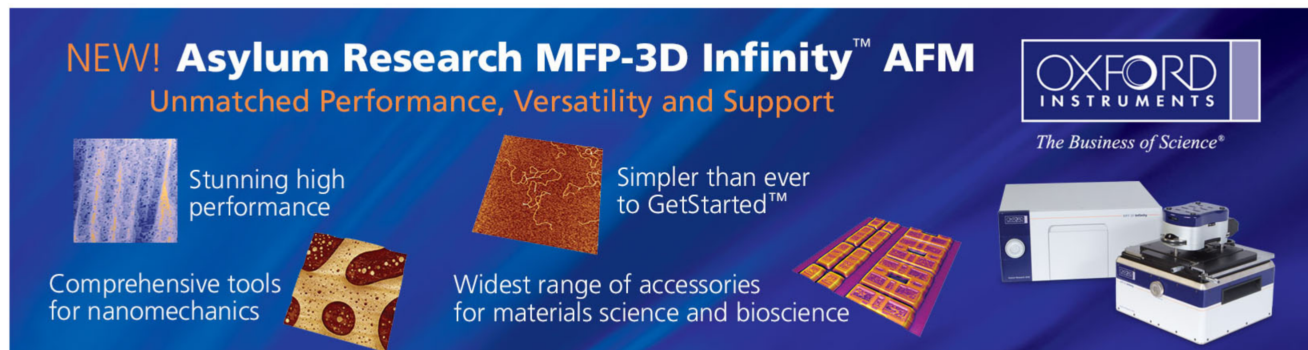

This article is copyrighted as indicated in the article. Reuse of AIP content is subject to the terms at: http://scitation.aip.org/termsconditions. Downloaded to IP: 140.113.38.11 On: Thu, 01 May 2014 02:41:45

Vanadium-doped indium tin oxide as hole-injection layer in organic light-emitting devices

T.-H. Chen
ULVAC Taiwan Inc., Taipei, Taiwan and Display Institute, National Chiao Tung University, Hsinchu, Taiwan

Y. Liou[a)]
Institute of Physics, Academia Sinica, Taipei, Taiwan

T. J. Wu and J. Y. Chen
ULVAC Taiwan Inc., Taipei, Taiwan

(Received 13 July 2005; accepted 4 October 2005; published online 8 December 2005)

Organic light-emitting devices were fabricated by using vanadium-doped indium tin oxide (ITO) as the hole-injection layers between the hole transport layer, N,N′-dia(1-napthl)-N,N′-diphenyl benzidine and the ITO anode. The vanadium-doped ITO layer was 15-nm thick with three different vanadium concentrations (6, 10.5, and 12.5 mol %). Three different resistivities (10, 500, and 10 000 Ω cm) and work functions (5, 5.2, and 5.4 eV) were obtained. The device with 6 mol % V-doped ITO layer possessing the least resistivity (10 Ω cm) and work function (5 eV) has the lowest turn-on voltage (below 3 V), the lowest operating voltage (below 7 V), the highest luminance (1000 cd/m^2 below 7 V), and the highest power efficiency (>5 lm/W at 10 mA/cm^2) among all. Such performance was attributed to the balance between the carrier concentration and the energy barrier for the hole injection. © *2005 American Institute of Physics*.
[DOI: 10.1063/1.2137892]

Organic light-emitting devices (OLEDs) with high brightness, high efficiency, full color, and low operating voltage have already been recognized as one of the future major flat panel displays. Highly transparent and conducting indium tin oxide (ITO) films have been the most commonly used anode on optoelectronic devices for a long time. Recent applications of ITO films as the anode for OLEDs have been widely reported.[1–5] A typical OLED consists of an ITO anode followed by a hole transport layer (HTL), a light emissive layer (LEL), an electron transport layer (ETL), and a metal cathode. Two organic materials, a typical HTL material, N,N′-bis-(1-naphthyl)-N,N′-diphenyl1-1,1-biphenyl 1-4, 4′-diamine (NPB), and the green LEL and ETL material, tris(8-hydroxyquinoline) aluminum (Alq_3), are commonly used in this structure. Charge injection from electrodes to organic materials plays an important role in the device performance. Usually, the mobility of the hole in the HTL is much higher than that of the electron in the ETL used in OLEDs. Reducing the number of holes in the HTL or enhancing electron injection in the ETL may help to improve electron-hole current balance in OLEDs. To modify the two electrodes is usually a common way to balance the current in OLEDs. The hole injection at the anode can be adjusted by different surface treatments as well as by inserting a buffer layer between the ITO and the HTL (Refs. 6–10). Oxygen plasma treatment of the ITO anode is the most common way to improve the device performance. In this way, both the contact resistance and the work function of the ITO anode have been increased due to the reduction of the oxygen deficiency near the surface.[11,12] It is well known that a layer of the copper phthalocyanine (CuPc) on the ITO anode can easily form a compact and smooth surface and dramatically enhance the device stability and performance.[13,14] The CuPc layer may enhance the hole injection by reducing the effective barrier between the ITO and the HTL but it may also decrease the hole-injection efficiency leading to a better balance of the charge's (holes and electrons) injection and recombination.[15] Various high work-function metals (Pt, Pd, etc.), insulating materials (Teflon, SiON), and oxides (SiO_2, transition-metal oxides, etc.) used as buffer layers on the ITO anode have demonstrated their capabilities of lowering the turn-on voltage, and enhancing the luminance efficiency and lifetime of OLEDs (Refs. 16–19). The improvement of the device performance was mostly attributed to the hole-injection enhancement which resulted from the energy barrier reduction between the ITO anode and the HTL by increasing the anode work function. For thin (~2 nm) oxide layers, the tunneling model was proposed and the barrier reduction was attributed to the band-bending mechanism. However, the hole may accumulate at the interface between the ITO anode and the oxide layer due to the non-Ohmic contact and these positive charges may suppress the hole injection from the ITO anode to the HTL. From our previous study, we have shown that the balance of the energy barriers from both sides of the hole-injection layer is also important to improve the device performance.[20] However, the balance between the hole injection and the hole suppression has not yet been clarified.

In this study, three different concentrations of vanadium were dope into the ITO as the buffer layer. Most of the doped vanadium in the ITO layer has been transformed into stable vanadium oxides (VO_x, VO_2, or V_2O_5), which is confirmed by the electron spectroscopy for chemical analysis (ESCA) method (the binding energy of $2P_{3/2}$ photoelectrons has a broadened peak about 516–517 eV). The uniformly doped VO_x in the ITO layer has reduced the oxygen deficiency and increased the resistivity. The lifetime of the device with the

[a)]Author to whom correspondence should be addressed; electronic mail: yung@phys.sinica.edu.tw

This article is copyrighted as indicated in the article. Reuse of AIP content is subject to the terms at: http://scitation.aip.org/termsconditions. Downloaded to IP: 140.113.38.11 On: Thu, 01 May 2014 02:41:45

 © 2005 American Institute of Physics

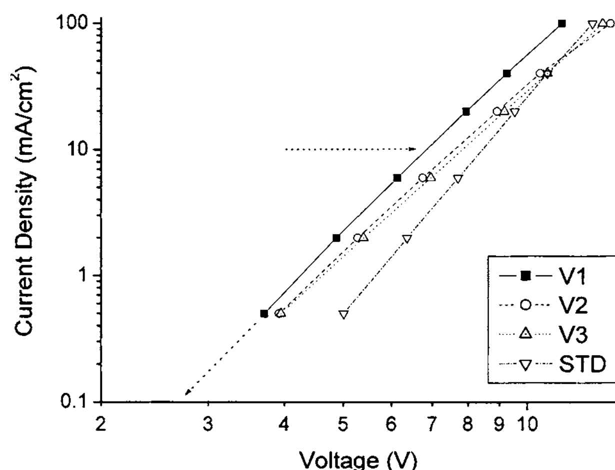

FIG. 1. The logarithmic plots of the current density-voltage curves of devices with V-doped ITO layers and the standard device.

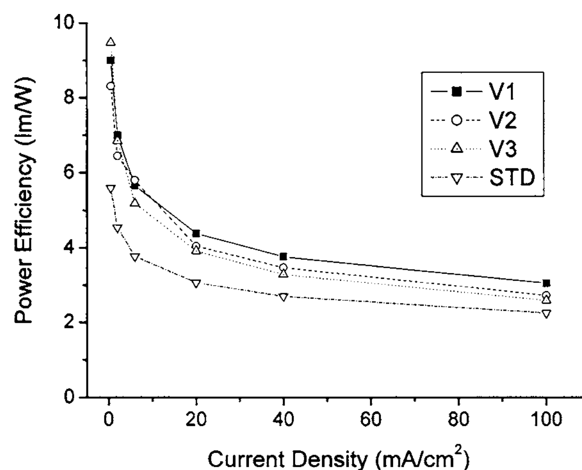

FIG. 3. The power efficiency–current density curves of devices with V-doped ITO layers and the standard device.

V-doped ITO layer has also been extended to about twice longer than that of the original device with pure ITO. Three different work functions and resistivies have been obtained. When compared with the low resistivity ($\sim 2\times10^{-4}$ Ω cm) of the undoped ITO anode, the high concentration (12%) V-doped ITO film has a large resistivity ($\sim$10 000 Ω cm) at room temperature, which makes it similar to an insulating oxide layer. The V-doped ITO layers with different work functions have different influences on the hole injection because the energy barriers between the ITO anode and the HTL have been changed. However, with the addition of a 15-nm-thick doping layer, there was no significant change ($<2\%$) on the transparency of the whole ITO film (155-nm thick). A green coumarin derivative, 10-(2-benzothiazolyl)-1,1,7,7-tetramethyl-2,3,6,7-tetrahydro-1H,5H,11H-benzo[l]pyrano[6,7,8–ij] quinolizin-11-one (C-545T), was doped in the light emissive layer (Alq_3) due to its good thermal stability and electroluminescence (EL) performance.[21] To compare and understand the significance of the device performance between the doped and undoped emissive layer, readers have to check with other previously published reports.[22,23]

ITO films about 140-nm thick with V-doped ITO layers (15 nm) were deposited on glass substrates by using a RF (for ITO) and dc (for V) cosputtering system. The ITO target is composed of $In_2O_3:SnO_2$ (9:1), and the V target is 99.9% pure. The base pressure in the system was approximately 1.0×10^{-6} Torr. The system pressure was about 5 mTorr during the film deposition. By controlling the gas flow rate, a gas mixture of about 8% of oxygen in argon was achieved. The substrate temperature was kept at 300 °C. To control the V contents in ITO, we changed the sputtering rate of each target. The concentrations and the uniformity of the V in ITO have been determined by both the Rutherford backscattering spectroscopy (RBS) and the secondary-ion-mass spectrometry (SIMS) depth profile. We have observed a constant V concentration in the doped ITO layer (15 nm) and a sharply decayed V profile ($<$20 nm) in the undoped ITO film. The work function of the V-doped ITO was determined by the commonly used ultraviolet photoelectron spectroscopy (UPS) method. The transmittance of the V-doped ITO (150 Å)/ITO (1400 Å) film was about 90% (at 550 nm). After the ITO (140 nm) film and the V-doped ITO layer (15 nm) are deposited, all organic layers, NPB (40 nm) and Alq_3 (40 nm) (doped with C545T), were deposited consecutively in vacuum by thermal evaporation with a base pressure of less than 10^{-7} Torr. Before and after the sample was transferred into the vacuum chamber, standard cleaning procedures (ultrasonic agitation in acetone and oxygen plasma sputtering) were applied. The influence of the oxygen plasma sputter cleaning on the work function of the V-doped ITO has been minimized by doing it quickly (5 min) and at a low power (100 W). For comparison, we have used a standard sample with a 15-nm-thick layer of CuPc (work function =5.2 eV) on top of the ITO film (140 nm) without the V-doped ITO layer by thermal evaporation during the device fabrication. The active area of the device was about 0.1 cm^2. These devices were completed with encapsulation in a dry argon glove box. The EL emission spectra and current-voltage-luminance characteristics were measured with a diode array rapid scan system using a Photo Research PR650 spectrophotometer and a computer-controlled dc source.

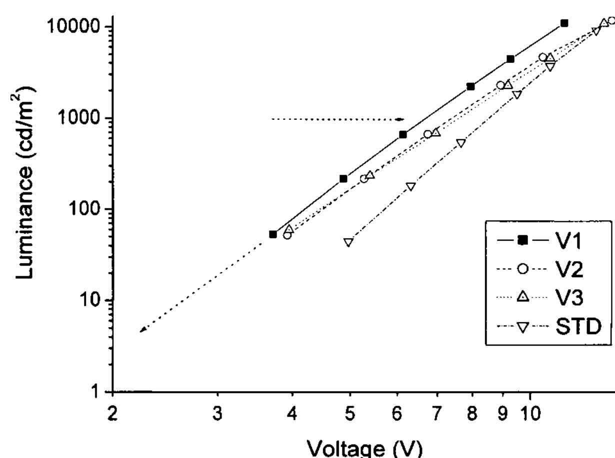

FIG. 2. The logarithmic plots of the luminance-voltage curves of devices with V-doped ITO layers and the standard device.

We have chosen three different concentrations (6, 10.5, and 12.5 mol %) of V (V1, V2, V3, respectively) to dope ITO films as buffer layers between the ITO anode and the HTL (NPB) to fabricate the EL devices. Since the vanadium metal is oxidized quickly in the film, we expected that the more the vanadium doped, the more the vanadium oxide formed. The resistivity at room temperature of these three different V-doped ITO layers increased from 2×10^{-4} Ω cm

This article is copyrighted as indicated in the article. Reuse of AIP content is subject to the terms at: http://scitation.aip.org/termsconditions. Downloaded to IP: 140.113.38.11 On: Thu, 01 May 2014 02:41:45

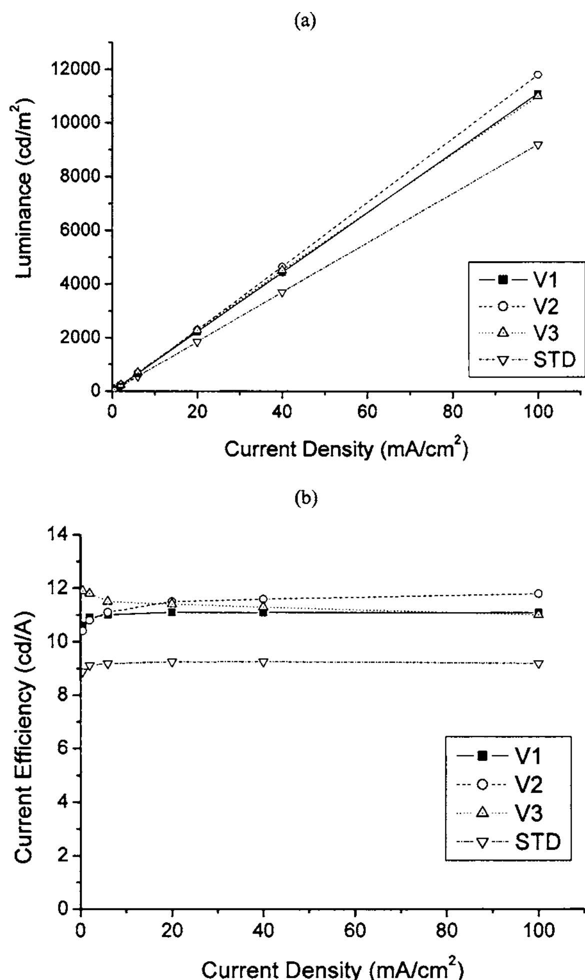

FIG. 4. (a) The luminance–current density curves of devices with V-doped ITO layers and the standard device. (b) The current efficiency-current density curves of devices with V-doped ITO layers and the standard device.

of undoped ITO to higher resistivities, 10 (V1), 500 (V2), and 10 000 (V3) Ω cm, respectively, due to the vanadium oxide formation. Since the resistivity–temperature curves have shown the semiconductor characteristics of the V-doped ITO layer, the resistivity was mainly determined by the carrier concentration. The work functions of these V-doped ITO layers were also increased from 4.7 eV of the undoped ITO anode to 5 (V1), 5.2 (V2), and 5.4 eV (V3), respectively. The increase of the resistivity and the work function have resulted in the lowering of the carrier concentration and the energy barrier for the hole injection. The current density–voltage curves clearly show that the device with the V1-doped ITO layer has the lowest turn-on (<3 V) and operating (<7 V) voltages, as shown in Figs. 1. The devices with V2- or V3-doped ITO layers have similar characteristics as the standard sample with CuPc buffer layer, because both the V2- and V3-doped ITO layers have relatively high resistivities and work functions as CuPc. This similarity was also observed in the luminance-current density curves, as shown in Figs. 2. The device with the V1-doped ITO layer has the EL luminance of 1000 cd/m^2 at an operating voltage below 7 V. From the power efficiency–current density curves, as shown in Fig. 3, the device with the V1-doped ITO layer has the power efficiency over 5 lm/W at a current density of 10 mA/cm^2. We attributed the best performance of the device with the V1-doped ITO layer to its relatively smaller resistivity and work function. If the energy barrier reduction was important to enhance the device performance, the device with the V3-doped ITO layer should have the best performance because it has the highest work function (5.4 eV). However, because the device with the V3-doped ITO layer has performed poorly, the hole injection must have been suppressed by the hole accumulation. If the balance of the energy barriers from both sides of the hole-injection layer is important, the best choice must be the device with the V2-doped ITO layer, which has a work function (5.2 eV) just between the work function of the ITO (4.7 eV) anode and that of the HTL (NPB, 5.7 eV). Actually, the device with the V2-doped ITO layer performed well in the luminance versus current density and the current efficiency versus current density, as shown in Figs. 4(a) and 4(b).

In summary, we have demonstrated that the performance of OLEDs has been improved by inserting a V-doped ITO layer as the hole-injection layer. The resistivity and the work function of the V-doped ITO layer were dependent on the vanadium concentrations. With a small work function (5 eV) and the lowest resistivity (10 Ω cm) of the 6 mol % V-doped ITO layer, the device has achieved a turn-on voltage below 3 V, an operating voltage below 7 V (at 10 mA/cm^2), a luminance of 1000 cd/m^2 below 7 V, and a power efficiency over 5 lm/W at 10 mA/cm^2. The balance between the carrier concentration and the energy barrier for hole injection was important for the best device performance.

[1]C. W. Tang and S. A. VanSlyke, Appl. Phys. Lett. **51**, 913 (1987).
[2]C. Adachi, T. Tsutsui, and S. Saito, Appl. Phys. Lett. **55**, 1489 (1989).
[3]C. W. Tang, S. A. VanSlyke, and C. H. Chen, J. Appl. Phys. **85**, 3610 (1989).
[4]R. H. Friend, R. W. Gymer, A. B. Holmes, J. H. Burroughes, R. N. Marks, C. Taliani, D. D. C. Bradley, D. A. Dos Santos, J. L. Bredas, M. Logdlund, and W. R. Salaneck, Nature (London) **397**, 121 (1999).
[5]J. Shi and C. W. Tang, Appl. Phys. Lett. **70**, 1665 (1997).
[6]C. Ganzorig, K.-J. Kwak, K. Yagi, and M. Fujihira, Appl. Phys. Lett. **79**, 272 (2001).
[7]W. Hu and M. Matsumura, Appl. Phys. Lett. **81**, 806 (2002).
[8]F. Zhang, A. Peter, and L. Dunsch, Appl. Phys. Lett. **82**, 4587 (2003).
[9]S. T. Zhang, X. M. Ding, J. M. Zhao, H. Z. Shi, J. He, Z. H. Xiong, H. J. Ding, E. G. Obbard, Y. Q. Zhan, W. Huang, and X. Y. Hou, Appl. Phys. Lett. **84**, 425 (2004).
[10]S. Y. Kim, J.-L. Lee, K.-B. Kim, and Y.-H. Tak, Appl. Phys. Lett. **86**, 133504 (2005).
[11]B. Low, F. Zhu, K. Zhang, and S. Chua, Appl. Phys. Lett. **80**, 4659 (2002).
[12]H. Y. Yu, X. D. Feng, D. Grozea, Z. H. Lu, R. N. Sodhi, A.-M. Hor, and H. Aziz, Appl. Phys. Lett. **78**, 2595 (2001).
[13]S. A. VanSlyke, C. H. Chen, and C. W. Tang, Appl. Phys. Lett. **69**, 2160 (1996).
[14]E. W. Forsythe, M. A. Abkowitz, Y. Gao, and C. W. Tang, J. Vac. Sci. Technol. A **18**, 1869 (2000).
[15]S. M. Tadayyon, H. M. Grandin, K. Griffiths, P. R. Norton, H. Aziz, and Z. D. Popovic, Org. Electron. **5**, 157 (2004).
[16]Y. Shen, D. B. Jacobs, G. G. Malliaras, G. Koley, M. G. Spencer, and A. Ioannodis, Adv. Mater. (Weinheim, Ger.) **13**, 1234 (2001).
[17]C. Qiu, H. Chen, Z. Xie, M. Wong, and H. S. Kwok, Appl. Phys. Lett. **80**, 3485 (2002).
[18]C. O. Poon, F. L. Wong, S. W. Tong, R. Q. Zhang, C. S. Lee, and S. T. Lee, Appl. Phys. Lett. **83**, 1038 (2003).
[19]J. Cui, Q. Huang, J. G. C. Veinot, H. Yan, and T. J. Marks, Adv. Mater. (Weinheim, Ger.) **14**, 565 (2002).
[20]T. H. Chen, Y. Liou, T. J. Wu, and J. Y. Chen, Appl. Phys. Lett. **85**, 2092 (2004).
[21]C. Chen and C. W. Tang, Appl. Phys. Lett. **79**, 3711 (2001).
[22]J. Littman and P. Martic, J. Appl. Phys. **72**, 1957 (1992).
[23]J. Kido and Y. Lizumi, Appl. Phys. Lett. **73**, 2721 (1998).

This article is copyrighted as indicated in the article. Reuse of AIP content is subject to the terms at: http://scitation.aip.org/termsconditions. Downloaded to IP: 140.113.38.11 On: Thu, 01 May 2014 02:41:45